

Discovery of $\text{Cs}_2(\text{UO}_2)\text{Al}_2\text{O}_5$ by Molten Flux Methods: A Uranium Aluminate Containing Solely Aluminate Tetrahedra as the Secondary Building Unit

Christian A. Juillerat,^{†,§} Vancho Kocovski,^{‡,§} Theodore M. Besmann,^{‡,§} and Hans-Conrad zur Loye^{*,†,§}

[†]Department of Chemistry and Biochemistry, University of South Carolina, Columbia, South Carolina 29208, United States

[‡]Nuclear Engineering Program, University of South Carolina, Columbia, South Carolina 29208, United States

[§]Center for Hierarchical Wasteform Materials (CHWM), University of South Carolina, Columbia, South Carolina 29208, United States

Supporting Information

ABSTRACT: The flux synthesis, solid state synthesis, and characterization of a new aluminate, $\text{Cs}_2(\text{UO}_2)\text{Al}_2\text{O}_5$, are reported. $\text{Cs}_2(\text{UO}_2)\text{Al}_2\text{O}_5$ crystallizes in the tetragonal space group $I4_1/amd$ with lattice parameters $a = 7.3254(2)$ and $c = 30.9849(7)$ and is constructed from edge-sharing chains of UO_7 pentagonal bipyramids that are connected to $[\text{Al}_2\text{O}_5]^{4-}$ two-dimensional sheets. The cesium cations, which are heavily disordered, occupy small channels in the a and b directions in the framework structure. The optical properties and ion exchange behaviors are reported along with DFT calculations that support the observed results of the ion exchange experiments.

The crystal chemistry of uranium continues to expand as nuclear energy and nuclear waste storage receive ongoing attention in the scientific community. The number of reported inorganic extended structures containing uranium has steadily grown from 180 well-refined published uranium(VI) containing structures in 1996, to 368 in 2005, and to 727 in 2016. Much of this data was summarized in the expansive hexavalent uranium structural reviews by Burns et al.^{1–3} In addition, uranium(IV) structures, while quite plentiful, are not nearly as widely reported as U(VI) structures. The recent expansion in our understanding of uranium crystal chemistry is mainly credited to exploratory crystal growth,⁴ which utilizes different combinations of reagents to incorporate the desired elements into the single-crystal products. This approach has resulted in a plethora of new, targeted structure types with new compositions as well as, at times, serendipitous results.

While uranium phosphates, arsenates, and silicates are well established classes of materials and flux growth of these materials is a well-established process, uranium germanates, by contrast, have only recently come into play as the number of flux grown uranium germanates increased from a single reported crystal structure in 2013 to 20 in 2018. Phosphate, arsenate, silicate, and germanate TO_4^{n-} units all commonly adopt tetrahedral coordination environments and have functioned as building blocks in compositionally diverse extended uranium structures; consequently, we decided to pursue other TO_4^{n-} tetrahedral

building blocks to achieve similar structures, specifically aluminum as AlO_4^{5-} . Aluminum commonly adopts a tetrahedral coordination environment when found in combination with highly electropositive cations and is well-known in the realm of zeolites and silicate minerals, where it substitutes on silicon sites.⁵ A simple ICSD search of U, Al, and O containing compounds yields 25 structures consisting of 18 minerals, one synthetic perovskite, one novel aluminoborate prepared by high temperature–high pressure methods,⁶ and five flux grown uranium aluminophosphates recently published by our group.⁷ Additionally, the synthesis of uranyl aluminate nanoparticles has also been reported.⁸ Herein, we report a novel cesium uranium aluminate, the first uranium extended structure to contain solely aluminate tetrahedra as the secondary building unit.

Crystals of $\text{Cs}_2(\text{UO}_2)\text{Al}_2\text{O}_5$ were initially obtained serendipitously from a flux reaction using 0.5 mmol of UF_4 (International Bio-Analytical Industries, powder, ACS grade), 0.33 mmol of LaPO_4 (Alfa Aesar, powder, 99.99%), 11 mmol of CsCl (Alfa Aesar, powder, 99.99%), and 9 mmol of CsF (Alfa Aesar, 99%) loaded into a silver tube covered loosely with a silver cap and held upright in the furnace with an alumina crucible. The mixture was heated to 875 °C in 1.5 h, held for 12 h, and slowly cooled to 400 °C at 6 °C/h. It appeared that the flux was not contained in the silver tube and reacted with the alumina crucible producing yellow crystals of the title compound on the rim of the alumina crucible (Figure 1). The reaction vessels were sonicated in water following removal from the furnace in order to loosen the crystals from the surface of the vessels by dissolving any remaining flux. All attempts to duplicate these conditions were unsuccessful, and these crystals could not be resynthesized using flux methods alone.

The structure and composition of $\text{Cs}_2(\text{UO}_2)\text{Al}_2\text{O}_5$ were determined by single-crystal X-ray diffraction, and this information was used to successfully synthesize the title compound by traditional solid state methods. Combining 0.5 mmol of $\text{UO}_2(\text{NO}_3)_2 \cdot 6 \text{H}_2\text{O}$ (International Bio-Analytical Industries, powder), 1 mmol of Al_2O_3 (Alfa Aesar, powder, 99.9%), and 1 mmol of CsNO_3 (Alfa Aesar, powder, 99.8%) into

Received: February 13, 2019

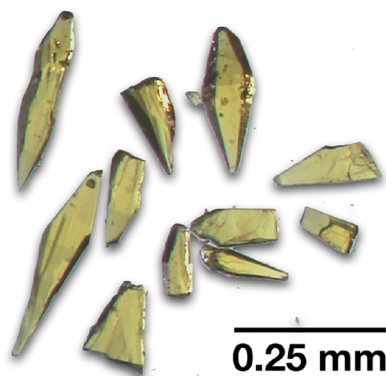


Figure 1. Optical images of single crystals of $\text{Cs}_2(\text{UO}_2)\text{Al}_2\text{O}_5$.

an alumina crucible and heating the mixture with intermittent grindings to 900 °C for 250 h, 950 °C for 48 h, 1000 °C for 96 h, and finally 1050 °C for 48 h resulted in the product phase. Between 900 and 1000 °C the target phase $\text{Cs}_2(\text{UO}_2)\text{Al}_2\text{O}_5$ forms together with $\text{Cs}_2\text{U}_2\text{O}_7$ (yellow), and at 1050 °C the target phase is present together with $\text{Cs}_4\text{U}_5\text{O}_{17}$ (orange). This mixture of $\text{Cs}_4\text{U}_5\text{O}_{17}$ and $\text{Cs}_2(\text{UO}_2)\text{Al}_2\text{O}_5$ was loaded into a platinum crucible with 9 mmol of CsF and 11 mmol of CsCl, and the resulting mixture was heated under the same conditions as the original flux reaction. These reaction conditions promoted the recrystallization of $\text{Cs}_4\text{U}_5\text{O}_{17}$ and $\text{Cs}_2(\text{UO}_2)\text{Al}_2\text{O}_5$ as orange plates and yellow crystals, respectively, that could be manually separated to obtain a relatively pure sample of $\text{Cs}_2(\text{UO}_2)\text{Al}_2\text{O}_5$. Powdered and single-crystalline products were identified by powder X-ray diffraction (PXRD) using a Bruker D2 Phaser equipped with an LXYENE silicon strip detector and a Cu K α source (Figure 2).

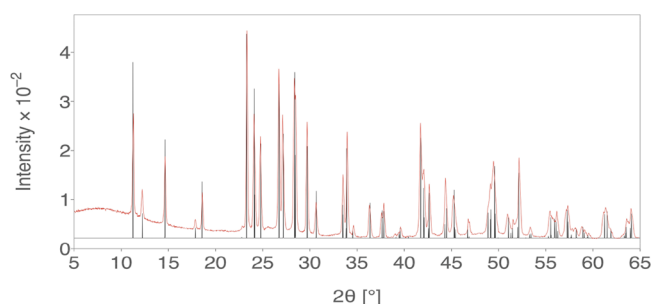


Figure 2. PXRD pattern of $\text{Cs}_2(\text{UO}_2)\text{Al}_2\text{O}_5$ (red) and the calculated pattern from the cif (black).

Single-crystal X-ray diffraction data were collected on a yellow plate crystal cut from the larger polyhedral crystals of $\text{Cs}_2(\text{UO}_2)\text{Al}_2\text{O}_5$ using a Bruker D8 Quest single-crystal X-ray diffractometer equipped with a Mo K α microfocus source ($\lambda = 0.71073 \text{ \AA}$). The structure of the single crystal was determined by reducing the data and applying an absorption correction using the SAINT+ and SADABS programs within APEX 3,⁹ solving using the SHELXT solution method, and refining the solution using SHELXL within the Olex 2 GUI.^{10–12} Full crystallographic data can be found in Table S1 along with bond distances and bond valence sums in Table S2. The refinement of the U, Al, and O sites was straightforward, while the refinement of the Cs sites, discussed further in the Supporting Information, was difficult due to the extreme disorder of the cations in the channels of the structures. As a result of the extreme disorder in

the Cs cations, diffuse scattering was visible in the diffraction frames of the single-crystal diffraction data (Figure S1). The final solution has an R_1 value of 1.69% and maximum/minimum electron density peaks of +0.9 and -1 , indicating the model of the Cs disorder matches well with the collected data; however, the positions and occupancies of the seven partially occupied cesium sites should be considered approximate. The elements in the structure solution were confirmed qualitatively by energy-dispersive spectroscopy (EDS) using a TESCAN Vega-3 SBU scanning electron microscope equipped with an EDS detector.

$\text{Cs}_2(\text{UO}_2)\text{Al}_2\text{O}_5$ crystallizes in the tetragonal space group $I4_1/amd$ with lattice parameters $a = 7.3254(2) \text{ \AA}$ and $c = 30.9849(7) \text{ \AA}$, where all sites lie on special positions. U1, O4, and Cs4 lie on Wyckoff site 8e with $2mm$ symmetry and O3 lies on Wyckoff site 16g with $.2$ symmetry, while all others lie on 16h with $.m$ symmetry. The structure of $\text{Cs}_2(\text{UO}_2)\text{Al}_2\text{O}_5$ consists of parallel 2D $[\text{Al}_2\text{O}_5]^{4-}$ sheets in the bc plane (Figure 3a) connected by chains of edge-sharing UO_7 square bipyramids. The 2D $[\text{Al}_2\text{O}_5]^{4-}$ sheets contain four-membered (vierer) and eight-membered (achter) rings where vierer rings are linked to form a layer through corner sharing so that only achter rings are formed between them. This aluminate sheet topology is similar to that of the silicate sheets found in $\text{K}_2[(\text{UO}_2)\text{Si}_4\text{O}_{10}]$, $\text{Na}_2(\text{UO}_2)-(\text{Si}_4\text{O}_{10})$, $\text{KNa}_3[(\text{UO}_2)_2(\text{Si}_4\text{O}_{10})_2]$, and $\text{Na}_4[(\text{UO}_2)_2(\text{Si}_4\text{O}_{10})_2]$ where the 2D nets are identical; however, the directions in which the tetrahedra point are different for all three structures.^{13–16}

This sheet topology is also observed in several aluminosilicate and silicate minerals such as paracelsian, feldspars, harmotome, philipsite, merlinoite, gismondine, garronite, and apophyllite, in addition to many other synthetic materials.¹⁷ Liebau explicitly lists the 29 different isomers of this simple topology that differ only by the direction that the tetrahedra point (up or down), of which only five have been observed to date. The title compound is, to our knowledge, the first example of no. 18.¹⁷ Figure 3b shows the connection of the aluminate sheets through edge-sharing on two sides of the equatorial planes of the pentagonal bipyramids, where the UO_7 chains alternate between the a and b directions between each aluminate sheet. The cesium atoms lie within the channels created by the gaps between parallel UO_7 chains.

As part of our interest in nuclear waste forms, first principle calculations were used to determine whether aqueous Cs^+ ion exchange with K^+ is energetically favorable. From the DFT+U calculated total energies (full details of these calculations can be found in the Supporting Information) we determined the energies for exchanging ion A with ion B ($A = \text{Cs}^+$, $B = \text{K}^+$), ΔE_{ie} , using the equation

$$\Delta E_{\text{ie}} = E_{\text{tot}}^{\text{B}} - E_{\text{tot}}^{\text{A}} + N\mu^{\text{A}} - N\mu^{\text{B}} \quad (1)$$

where $E_{\text{tot}}^{\text{A}}$ and $E_{\text{tot}}^{\text{B}}$ are the total energy of the system containing ion A and B, respectively, μ^{A} and μ^{B} are the chemical potential of the A and B ions, respectively, and N is the total number of ions being exchanged, in our case 16. For comparison purposes we used the chemical potential of the ions in vacuum and in water. The calculated ΔE_{ie} are negative, $-0.531 \text{ eV/exchanging ion in a vacuum}$ and $-0.140 \text{ eV/exchanging ion in water}$, indicating a strong driving force for exchanging Cs^+ ions with K^+ .

Ion exchange experiments were performed both on single-crystal and ground crystalline samples by soaking 20 mg samples in 4 m KCl for 3 days at 90 °C without stirring. A control experiment was performed by soaking $\text{Cs}_2(\text{UO}_2)\text{Al}_2\text{O}_5$ in water at 90 °C for 4 days. After the experiments, the single crystals

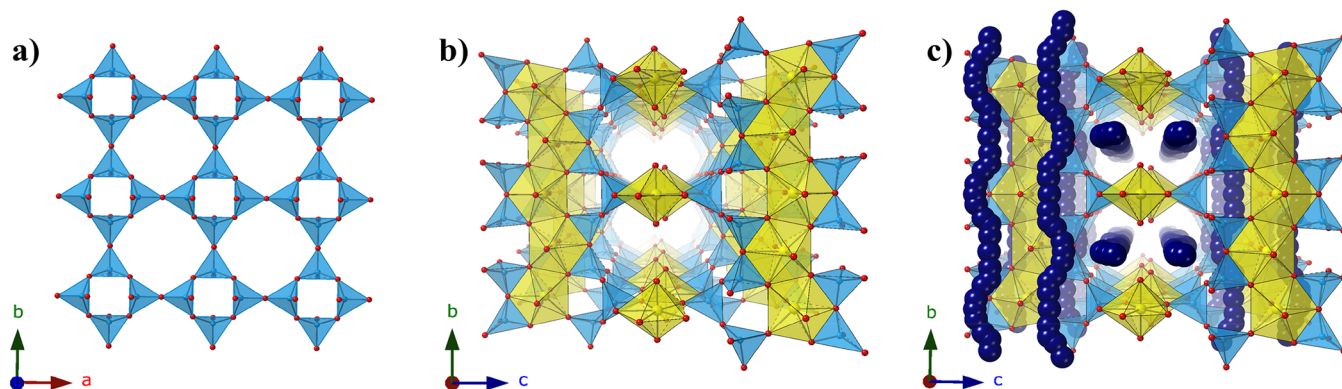


Figure 3. (a) 2D aluminate sheet constructed of vierer and achter rings. (b) Aluminate sheets connected by edge sharing chains of UO_7 polyhedra. (c) $\text{Cs}_2(\text{UO}_2)\text{Al}_2\text{O}_5$ shown with all sites. Uranyl polyhedra are yellow, aluminate tetrahedra blue, cesium cations in dark blue, and oxygen atoms in red.

were no longer single crystalline but rather had transformed into a polycrystalline powder. The control experiment showed no significant change in the PXRD pattern, indicating the stability of $\text{Cs}_2(\text{UO}_2)\text{Al}_2\text{O}_5$ in water over the short period of 4 days. The powder ion exchange product was analyzed by EDS and PXRD methods described previously and support near complete exchange of Cs for K. A calculated pattern for the K bearing ion exchange product was obtained by replacing the Cs sites with K and refining the lattice parameters in Jade 9, which resulted in lattice parameters $a = 7.2165(7)$ Å and $c = 30.323(7)$ Å.¹⁸ The DFT+*U* calculations well reproduce the change in lattice parameter when Cs is completely exchanged by K (see Table S4). The experimental and calculated patterns are shown in Figure 4 and demonstrate a good fit. There are unidentified

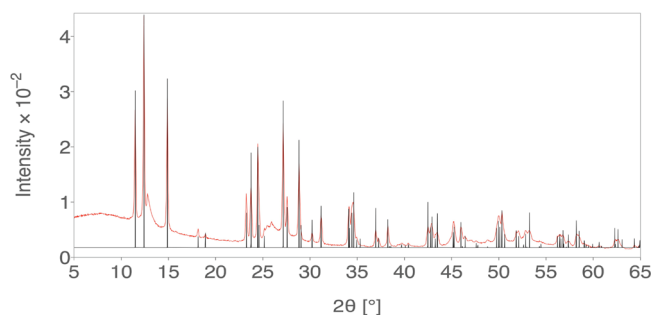


Figure 4. Experimental PXRD pattern of the K ion exchange product (red) and the calculated pattern (black).

peaks at approximately 13° and 26° 2θ that were not present in the PXRD prior to ion exchange and are possibly a result of some decomposition. Our experimental results support the DFT calculations that predicted the exchange of Cs^+ to K^+ is energetically favorable.

Optical measurements on $\text{Cs}_2(\text{UO}_2)\text{Al}_2\text{O}_5$ were performed using a PerkinElmer Lambda 35 UV–vis spectrometer equipped with an integrating sphere and a PerkinElmer LS55 luminescence spectrometer. The UV–vis diffuse-reflectance data were collected over 200–900 nm and converted internally using the Kubelka–Munk equation.¹⁹ $\text{Cs}_2(\text{UO}_2)\text{Al}_2\text{O}_5$ absorbs broadly from 200 to 530 nm, classifying the title compound as a semiconductor, with the charge transfer band centered at 354 nm and the UO_2^{2+} transitions at 435 and 446 nm with a shoulder at 505 nm (Figure 5a). The DFT+*U* calculations show that the title compound is specifically a charge-transfer insulator (see Figure S2), unlike UO_2 and the previously studied uranyl

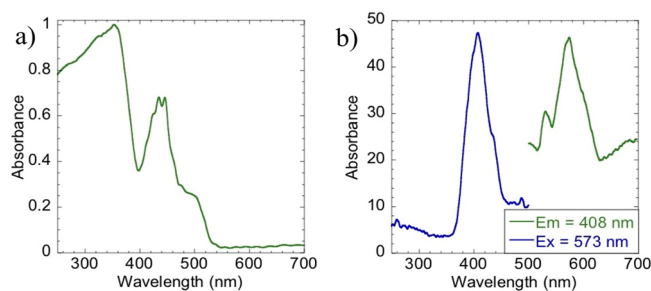


Figure 5. (a) Normalized UV–vis spectra and (b) fluorescence excitation and emission spectra of $\text{Cs}_2(\text{UO}_2)\text{Al}_2\text{O}_5$.

phosphates,²⁰ with a slightly larger band gap of 423 nm. Replacing P with the less electronegative element, Al, makes the $\text{Cs}_2(\text{UO}_2)\text{Al}_2\text{O}_5$ system more ionic, pushing the O states to higher energies; consequently, the states at the top of the valence band are exclusively from the O atoms. The maximum fluorescence emission occurs when exciting at 408 nm, and the maximum peak of the emission spectrum is at 573 nm with a smaller peak at 530 nm, which is typical of UO_2^{2+} fluorescence (Figure 5b). While the fluorescence emission spectra is typical of solid state UO_2^{2+} species, the UV–vis diffuse reflectance data are unusual in the fact that the vibronically coupled transitions of the UO_2^{2+} are significantly narrower than in spectra of other recently reported solid state UO_2^{2+} species.^{7,21–25}

In summary, the first uranium material solely containing aluminum tetrahedra as the secondary building unit was discovered serendipitously by molten flux methods and synthesized by combined solid state and flux methods. The structure was characterized by SXR, PXRD, EDS, optical spectroscopy, and modeled by DFT calculations to determine the feasibility of the exchange of Cs^+ cations for K^+ in water. The ion exchange reaction was shown to be favorable by DFT+*U* calculations, which was supported by our analysis of the ion exchange product that was confirmed to have exchanged essentially all Cs^+ for K^+ and to have a similar powder pattern that can be indexed with unit cell parameters similar to those of the parent phase. This work demonstrates the ability to form uranium aluminates by molten flux methods, although the exact reaction conditions that produced this phase are poorly understood and should be the subject of future investigations in order to expand this new class of uranium aluminate materials.

ASSOCIATED CONTENT

Supporting Information

The Supporting Information is available free of charge on the ACS Publications website at DOI: 10.1021/acs.inorgchem.9b00435.

Crystallographic refinement details, tables of crystallographic information, diffraction frame from the single-crystal X-ray data, select bond distances, bond valence sums, additional details on the DFT calculations, total and partial DOS (PDF)

Accession Codes

CCDC 1894955 contains the supplementary crystallographic data for this paper. These data can be obtained free of charge via www.ccdc.cam.ac.uk/data_request/cif, or by emailing data_request@ccdc.cam.ac.uk, or by contacting The Cambridge Crystallographic Data Centre, 12 Union Road, Cambridge CB2 1EZ, UK; fax: +44 1223 336033.

AUTHOR INFORMATION

Corresponding Author

*E-mail: zurloye@mailbox.sc.edu.

ORCID

Christian A. Juillerat: 0000-0002-8270-1964

Vancho Kocovski: 0000-0002-2127-5834

Hans-Conrad zur Loye: 0000-0001-7351-9098

Author Contributions

The manuscript was written through contributions of all authors. All authors have given approval to the final version of the manuscript.

Notes

The authors declare no competing financial interest.

ACKNOWLEDGMENTS

Research was conducted by the Center for Hierarchical Wasteform Materials (CHWM), an Energy Frontier Research Center (EFRC). Research was supported by the U.S. Department of Energy, Office of Basic Energy Sciences, Division of Materials Sciences and Engineering under Award DE-SC0016574. C. Juillerat is additionally supported by an NSF IGERT Graduate Fellowship under grant number 1250052.

REFERENCES

- (1) Lussier, A. J.; Lopez, R. A. K.; Burns, P. C. A revised and expanded structure hierarchy of natural and synthetic hexavalent uranium compounds. *Can. Mineral.* **2016**, *54*, 177–283.
- (2) Burns, P. C. U^{6+} minerals and inorganic compounds: insights into an expanded structural hierarchy of crystal structures. *Can. Mineral.* **2005**, *43*, 1839–1894.
- (3) Burns, P. C.; Ewing, R. C.; Hawthorne, F. C. The crystal chemistry of hexavalent uranium: polyhedron geometries, bond-valence parameters, and polymerization of polyhedra. *Can. Mineral.* **1997**, *35*, 1551–1570.
- (4) Juillerat, C. A.; Klepov, V. V.; Morrison, G.; Pace, K. A.; zur Loye, H.-C. Flux Crystal Growth: A Versatile Technique to Reveal the Crystal Chemistry of Complex Uranium Oxides. *Dalton Trans* **2019**, *48*, 3162.
- (5) Santamaría-Pérez, D.; Vegas, A. The Zintl-Klemm concept applied to cations in oxides. I. The structures of ternary aluminates. *Acta Crystallogr., Sect. B: Struct. Sci.* **2003**, *B59*, 305–323.
- (6) Wu, S.; Beermann, O.; Wang, S.; Holzheid, A.; Depmeier, W.; Malcherek, T.; Modolo, G.; Alekseev, E. V.; Albrecht-Schmitt, T. E. Synthesis of Uranium Materials under Extreme Conditions:

$UO_2[B_3Al_4O_{11}(OH)]$, a Complex 3D Aluminoborate. *Chem. - Eur. J.* **2012**, *18*, 4166–4169.

- (7) Juillerat, C. A.; Klepov, V. V.; Alekseev, E. V.; zur Loye, H.-C. Overstepping Lüwenstein's Rule – a Route to Unique Aluminophosphate Frameworks with 3D Salt-Inclusion and Ion Exchange Properties. *Inorg. Chem.* **2019**, *58*, 724–736.

- (8) Chave, T.; Nikitenko, S. I.; Scheinost, A. C.; Berthon, C.; Arab-Chapelet, B.; Moisy, P. First synthesis of uranyl aluminate nanoparticles. *Inorg. Chem.* **2010**, *49*, 6381–6383.

- (9) Bruker. APEX3, SAINT+, and SADABS; Bruker AXS Inc.: Madison, Wisconsin, USA, 2015.

- (10) Sheldrick, G. M. Crystal structure refinement with SHELXL. *Acta Crystallogr., Sect. C: Struct. Chem.* **2015**, *C71*, 3–8.

- (11) Sheldrick, G. M. SHELXT - Integrated space-group and crystal-structure determination. *Acta Crystallogr., Sect. A: Found. Adv.* **2015**, *A71*, 3–8.

- (12) Dolomanov, O. V.; Bourhis, L. J.; Gildea, R. J.; Howard, J. A. K.; Pushmann, H. OLEX2: a complete structure solution, refinement and analysis program. *J. Appl. Crystallogr.* **2009**, *42*, 339–341.

- (13) Liu, H.-K.; Peng, C.-C.; Chang, W.-J.; Lii, K.-H. Tubular Chains, Single Layers, and Multiple Chains in Uranyl Silicates: $A_2[(UO_2)_2Si_4O_{10}]$ ($A = Na, K, Rb, Cs$). *Cryst. Growth Des.* **2016**, *16*, 5268–5272.

- (14) Wang, X.; Huang, J.; Liu, L.; Jacobson, A. J. The novel open-framework uranium silicates $Na_2(UO_2)(Si_4O_{10}) \cdot 2.1H_2O$ (USH-1) and $RbNa(UO_2)(Si_2O_6) \cdot H_2O$ (USH-3). *J. Mater. Chem.* **2002**, *12*, 406–410.

- (15) Burns, P. C.; Olson, R. A.; Finch, R. J.; Hanchar, J. M. $KNa_3(UO_2)_2(Si_4O_{10})(H_2O)_4$, a new compound formed during vapor hydration of an actinide-bearing borosilicate waste glass. *J. Nucl. Mater.* **2000**, *278*, 290–300.

- (16) Li, Y.; Burns, P. C. The structures of two sodium uranyl compounds relevant to nuclear waste disposal. *J. Nucl. Mater.* **2001**, *299*, 219–226.

- (17) Liebau, F. *Structural Chemistry of Silicates: Structure, Bonding, and Classification*; Springer-Verlag: Berlin, 1985.

- (18) Jade, version 9.6.0; PXRD analysis software; Materials Data, Inc.: Livermore, CA, 2014.

- (19) Kubelka, P.; Munk, F. Z. Ein Beitrag Zur Optik Der Farbanstriche. *Z. Techn. Phys.* **1931**, *12*, 593–601.

- (20) Kocovski, V.; Juillerat, C. A.; Moore, E. E.; zur Loye, H.-C.; Besmann, T. Understanding the polymorphism of $A_4[(UO_2)_3(PO_4)_2O_3]$ ($A = \text{alkali metals}$) uranyl phosphate framework structures. *Cryst. Growth Des.* **2019**, *19*, 966–975.

- (21) Juillerat, C. A.; Moore, E. E.; Morrison, G.; Smith, M. D.; Besmann, T. M.; zur Loye, H.-C. Versatile Uranyl Germanate Framework Hosting Twelve Different Alkali Halide 1D Salt Inclusions. *Inorg. Chem.* **2018**, *57*, 11606–11615.

- (22) Juillerat, C. A.; Moore, E. E.; Besmann, T. B.; zur Loye, H.-C. Observation of an Unusual Uranyl Cation-Cation Interaction in the Strongly Fluorescent Layered Uranyl Phosphates $Rb_6[(UO_2)_7O_4(PO_4)_4]$ and $Cs_6[(UO_2)_7O_4(PO_4)_4]$. *Inorg. Chem.* **2018**, *57*, 3675–3678.

- (23) Juillerat, C. A.; Moore, E. E.; Kocovski, V.; Besmann, T. M.; zur Loye, H.-C. A Family of Layered Phosphates Crystallizing in a Rare Geometrical Isomer of the Phosphuranyl Topology: Synthesis, Characterization, and Computational Modeling of $A_4[(UO_2)_3O_2(PO_4)_2]$ ($A = \text{alkali metals}$) Exhibiting Intra-layer Ion Exchange. *Inorg. Chem.* **2018**, *57*, 4726–4738.

- (24) Morrison, G.; Smith, M. D.; Tran, T. T.; Halasyamani, S.; zur Loye, H.-C. Synthesis and structure of the new pentary uranium(VI) silicate, $K_4CaUSi_4O_{14}$, a member of a structural family related to frenoite. *CrystEngComm* **2015**, *17*, 4218–4224.

- (25) Read, C. M.; Yeon, J.; Smith, M. D.; zur Loye, H.-C. Crystal growth, structural characterization, cation-cation interaction classification, and optical properties of uranium (vi) containing oxychlorides, $A_4U_5O_{16}Cl_2$ ($A = K, Rb$), $Cs_5U_7O_{22}Cl_3$, and AUO_3Cl ($A = Rb, Cs$). *CrystEngComm* **2014**, *16*, 7259.